

Washington University in St. Louis

Washington University Open Scholarship

Mechanical Engineering and Materials Science
Independent Study

Mechanical Engineering & Materials Science

4-1-2022

A Simple Model of Thermal Insulation Design for Cryogenic Liquid Hydrogen Tank

Claire McFarland

Washington University in St. Louis

Ramesh K. Agarwal

Washington University in St. Louis

Follow this and additional works at: <https://openscholarship.wustl.edu/mems500>

Recommended Citation

McFarland, Claire and Agarwal, Ramesh K., "A Simple Model of Thermal Insulation Design for Cryogenic Liquid Hydrogen Tank" (2022). *Mechanical Engineering and Materials Science Independent Study*. 176. <https://openscholarship.wustl.edu/mems500/176>

This Final Report is brought to you for free and open access by the Mechanical Engineering & Materials Science at Washington University Open Scholarship. It has been accepted for inclusion in Mechanical Engineering and Materials Science Independent Study by an authorized administrator of Washington University Open Scholarship. For more information, please contact digital@wumail.wustl.edu.

MEMS 500: Independent Study Report

A simple Model of Thermal Insulation Design for Cryogenic Liquid Hydrogen Tank

Claire McFarland and Ramesh K. Agarwal

Abstract

A plane is being designed that will be similar in size and range to a Boeing 787-800 that will run on hydrogen fuel. The hydrogen will be stored cryogenically as a liquid in external fuel tanks located on the wings. The fuel tanks require insulation to maintain cryogenic conditions and prevent excessive boiloff of hydrogen and pressure buildup within the fuel tanks. This report details a one-dimensional, steady-state analysis of the heat transfer across the tank structure to determine the relationship between the thickness of the insulation layer on the tank and the boiloff rate of the liquid hydrogen. Expanded Polystyrene (EPS) was determined to be the best insulation material, and at cruise conditions of 35,000 ft, required an insulation thickness of 3.97 inches and weight of 624 lbs per tank to maintain a boiloff rate below 50% of the idle fuel usage rate. At on-ground idle conditions on a hot day, EPS was found to require an insulation thickness 1.37 inches and weight of 191 lbs per tank to maintain a boiloff rate below 50% of the idle fuel usage rate.

Introduction

It is important for the hydrogen tanks to be well insulated because excessive boiloff (evaporation) of the liquid hydrogen can lead to dangerous pressure buildup in the tank that could cause damage to the tank structure and possibly leaks or an explosion. To mitigate these dangerous effects, a pressure valve that allows the release of hydrogen gas when the tank exceeds a safe pressure must be included in the design. However, releasing hydrogen from the tank is inefficient because it is a loss of fuel that has weight and volume that the plane has been required to carry from the start of its journey. Additionally, releasing hydrogen into the atmosphere is an enabler for the creation of greenhouse gases.¹ So, it is best to insulate the tanks to reduce the boiloff of hydrogen. Since weight savings are very important for aircraft, the insulation should be designed to have a minimal weight while still reducing the hydrogen boiloff rate to the desired level.

The thermal loads that the tank will be subject to which are considered in this model are the forced convection on the outer surface of the tank, radiation due to the temperature differential between the tank surface and the surrounding air, incident solar radiation, and conduction through the layers of the tank structure as well as the lugs which connect the tank to the wing.

The following equations are used to calculate the thickness of the insulation based off a given boiloff rate. Equation 1 gives the formula to find the heat transfer across a system of one or more elements using the temperatures on either side of the system as well as the equivalent thermal resistance of the system.²

$$Q = \frac{T_1 - T_2}{R_{eq}} \quad [1]$$

Equation 2 shows how to calculate the thermal resistance to conduction across an element of thickness t with thermal conductivity k and cross-sectional area A .²

$$R_k = \frac{t}{kA} \quad [2]$$

Equation 3 shows how to calculate the heat flow due to incident solar radiation with the absorptivity of the surface α , the incident solar flux Q_{sol} , and the perpendicular/projected area of the surface A .²

$$Q = \alpha Q_{sol} A \quad [3]$$

Equation 4 shows how to calculate the radiative heat flow between a small object surrounded by a medium at a different temperature. α is the absorptivity of the surface, sigma is the Stefan Boltzmann constant, A is the surface area of the small object, and T_1 and T_2 are the surface temperature of the small object and the temperature of the surroundings respectively.²

$$Q = \alpha \sigma A (T_1^4 - T_2^4) \quad [4]$$

Equations 5-7 and 11-12 are used to calculate the heat flow due to forced convection across a cylinder. Equation 5 gives the Reynolds number as a function of the fluid density, fluid velocity, characteristic length (cylinder diameter), and fluid dynamic viscosity.²

$$Re = \frac{\rho v D}{\mu} \quad [5]$$

Equation 6 gives the Prandtl number as a function of the fluid heat capacity, fluid dynamic viscosity, and fluid thermal conductivity.²

$$Pr = \frac{c_p \mu}{k} \quad [6]$$

Equation 7 gives the Nusselt number for forced convection across a flat plate as a function of the Reynolds and Prandtl numbers.²

$$Nu = 0.644 Re^{1/2} Pr^{1/3} \quad [7]$$

Equations 8-12 are used to calculate the heat flow due to natural convection off a horizontal cylinder. Equation 8 gives the Grashof number as a function of gravity, the fluid thermal expansion

coefficient, the temperature differential between the surface and its surroundings, the length of the cylinder, and the fluid dynamic viscosity.²

$$Gr = \frac{g\beta(T_s - T_\infty)L^3}{\mu} \quad [8]$$

Equation 9 gives the Rayleigh number as a function of the Grashof number and the fluid Prandtl number.²

$$Ra = Gr * Pr \quad [9]$$

Equation 10 gives the Nusselt number for natural convection off a horizontal cylinder as a function of the Rayleigh number and the Prandtl number.²

$$Nu = \left\{ 0.60 + \frac{0.387Ra^{1/6}}{[1 + (0.559/Pr)^{9/16}]^{8/27}} \right\}^2 \quad [10]$$

Equation 8 gives the convection coefficient as a function of the Nusselt number, the thermal conductivity of the solid, and the characteristic length (cylinder length).²

$$h = \frac{Nu*k}{L} \quad [11]$$

Equation 9 gives the heat flow as a function of the convection coefficient, surface area of the cylinder, and temperature differential between the surface of the cylinder and the air.²

$$Q = hA(T_1 - T_2) \quad [12]$$

Equations 10 and 11 show how thermal resistances can be summed in series or in parallel to find equivalent resistances of systems with more than one element.²

$$series(R_1 \rightarrow R_n) = \sum_{i=1}^n R_i \quad [13]$$

$$parallel(R_1 \rightarrow R_n) = [\sum_{i=1}^n R_i^{-1}]^{-1} \quad [14]$$

The insulation materials that will be investigated in this report are Expanded Polystyrene (EPS), Multi-Layer Insulation (MLI), and Glass Bubbles insulation. EPS, also known as Styrofoam, has a thermal conductivity of 0.02594 W/m*K and a density of 1.6229 lbs/ft³.³ MLI is a very new technology that it still in the research and development phase. It consists of multiple layers of highly reflective material with highly insulating spacers sandwiched between them. There is limited data on its performance, particularly at cryogenic temperatures. Generally, MLI excels at reflecting radiation but is not particularly insulating against conduction and convection.⁴ MLI's conduction resistance is greatly increased when it is contained in a vacuum layer, but it requires a lot of energy to create and maintain a vacuum. For this application, the MLI will not be contained in a vacuum because it would significantly increase the cost of installation and maintenance. Instead, the MLI for this application will have solid layers of EPS in between the layers of reflective-coated mylar.⁵ This study assumes that the MLI has a

low thermal conductivity of $0.135 \cdot 10^{-3} \text{ W/m} \cdot \text{K}$ for radiation loads, and a thermal conductivity equal to that of EPS for conduction and convection loads. This MLI has a density of 10.8 lbs/ft^3 .⁶ Glass Bubbles insulation is made of small, hollow glass spheres that can be poured into a space to fill it. It has a thermal conductivity of $0.130 \text{ W/m} \cdot \text{K}$ and a density of 14.36 lbs/ft^3 .⁷ Although it has a higher thermal conductivity than EPS or MLI, its completely flexible structure has benefits for installing and maintaining insulation layers as well as managing mechanical stresses due to thermal loads.

Methods

Figure 1 shows the schematic diagram of the cylindrical fuel tank with insulation layers.

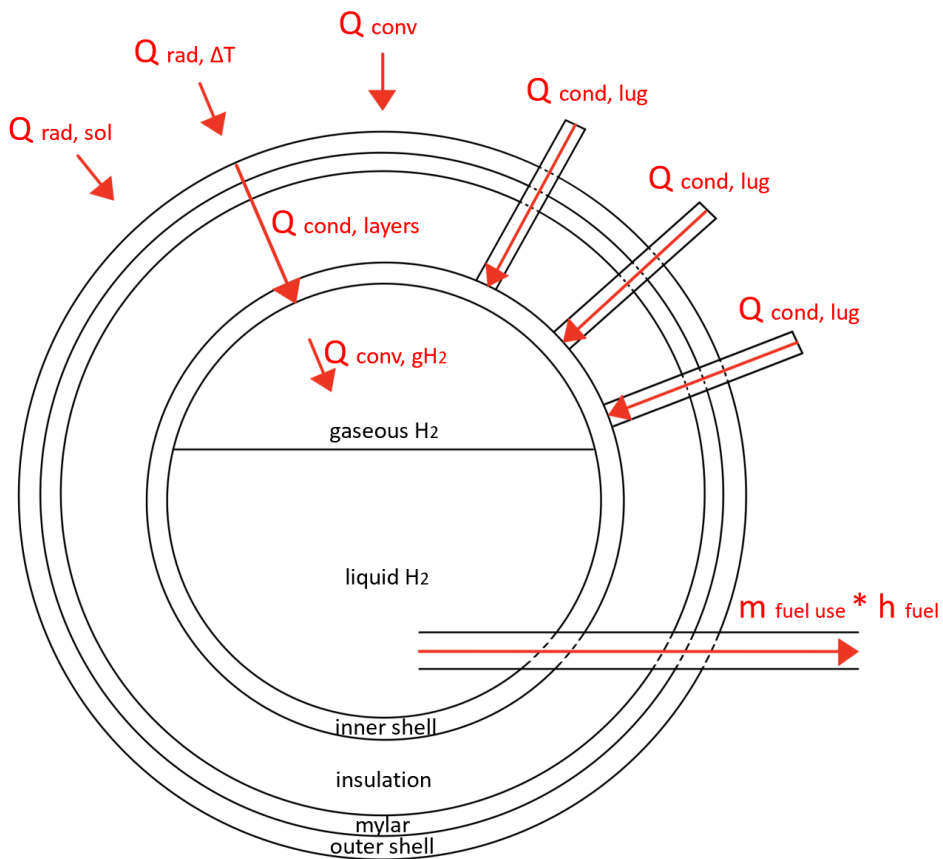


Figure 1: Schematic diagram of the cylindrical fuel tank with insulation layers.

On the outside of the tank, there is radiation heat transfer due to the solar irradiation incident on the surface, radiation due to the temperature differential between the air and the tank surface, and convection heat transfer (either forced convection in flight or natural convection on the ground while stationary). The conductive heat transfer through the outer shell layer, mylar layer, insulation layer, structural shell, and the lugs is also considered. The heat loss due to fuel usage is also considered. A close-up of one of the three identical lugs is shown in Figure 2 below.

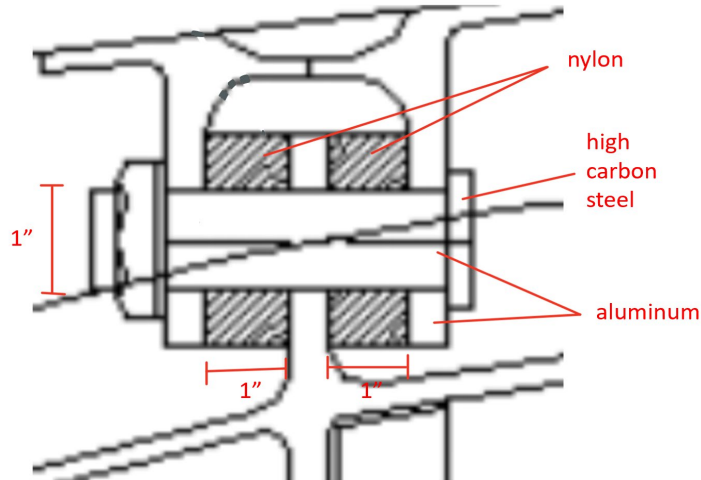


Figure 2: Schematic of one of the three identical lugs

A diagram showing this heat transfer model in Figure 1 as a thermal resistance network, which is analogous to an electric circuit, is shown in Figure 3. Every solid dot represents a surface with a temperature of interest, every line with a triangle on it represents a heat flux, and the rest of the lines show pathways for heat flow with a resistor representing the thermal resistance across a specific element (k for conduction resistance, h for convection resistance).

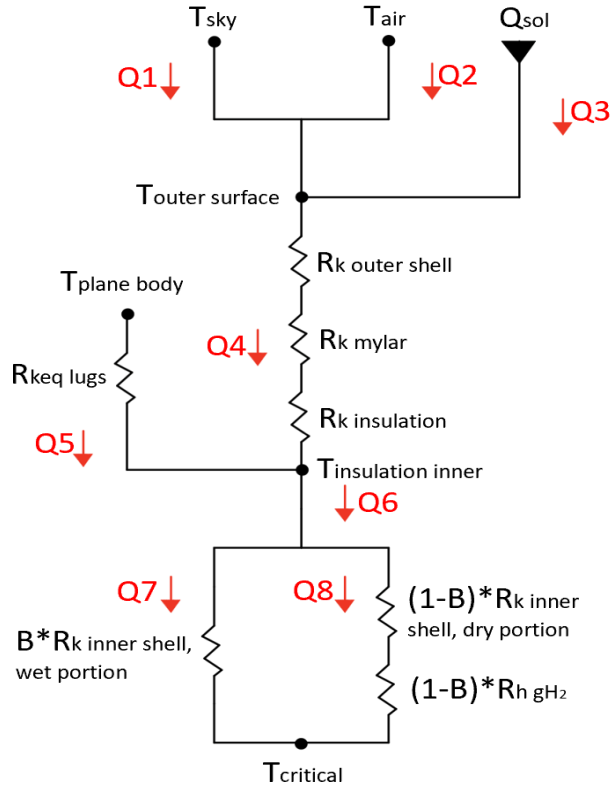


Figure 3: Thermal resistance network analogous to an electric circuit

The bottom split in Figure 3 accounts for when the tank begins to empty and gaseous hydrogen fills the space above the level of remaining liquid hydrogen. The left path, Q7, represents conductive heat flow through the portion of the structural shell which is in contact with the liquid hydrogen. The right path, Q8, represents the conductive heat flow through the portion of the structural shell which is in contact with the gaseous hydrogen and the convective heat flow through the gaseous hydrogen to the liquid hydrogen below. The variable beta is used to give a proportion between the two paths depending on how full the tank is, e.g. when it is full of liquid hydrogen, beta equals 1, so that Q8 equals 0. The value of beta is not straightforward to calculate as the tank level decreases, but it can be assumed to be close to 0 when the tank is almost empty. Instead of performing a continuous analysis of the heat transfer as the tank goes from full to empty. We are therefore picking discrete cases when the tank is full and nearly empty.

Q5, spanning from the plane body to the inside of the insulation, is the conduction heat flow through the lugs, with an equivalent resistance for the three lugs used. A detailed thermal resistance network diagram of one of the lugs, showing how to calculate this equivalent thermal resistance, is shown in Figure 4. It looks at just the left half of the lug, assuming the lug can be modeled as symmetrical about the central vertical axis, so the result from the model below can just be multiplied by 2 to get the total equivalent resistance of the lug.

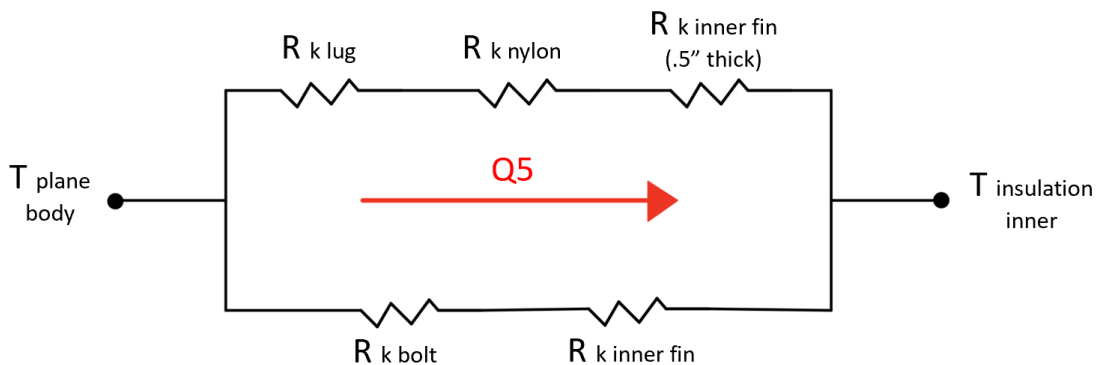


Figure 4: Detailed thermal resistance network diagram of one of the lugs

The thermal conductivity of the MLI is different for conduction and convection versus radiation heat loads. Since all three of these heat transfers are combined into one total heat transfer in this model, the thermal conductivity of the MLI is calculated as a function of the ratio of conduction and convection to radiation heat loads.

A conservation of energy equation looking at the inside of the structural shell as the control volume gives the following equations:

$$Q_{in} - Q_{out} = \dot{m}_{boiloff} h_{fg} \quad (15)$$

$$Q_7 + Q_8 = \dot{m}_{boiloff} h_{fg} \quad (16)$$

The mass flow of hydrogen out of the tank for fuel usage is not included in the energy conservation equation because this mass flow is generated by a pump which does work on the system equivalent to the energy of the mass flow, cancelling out these two parameters. If a numerical boiloff rate is assumed, the value of $Q_7 + Q_8$ can be determined. For now, we will assume that the tank is full of liquid hydrogen, therefore Q_8 is equal to 0. The temperature of the outside surface of the structural shell can now be obtained from equations [1] and [2]. The equivalent resistance of the three lugs can be calculated using equations [2], [13], and [14]. The heat transfer across the three lugs can then be calculated using equation [1]. Q_4 can now be found since from conservation of energy $Q_4 + Q_5 = Q_7 + Q_8$. The radiative heat transfer due to incident solar irradiation, Q_3 , can be found using equation [3]. The radiative heat transfer due to the temperature differential between the tank outer surface and the air, Q_1 , can be found using equation [4], leaving the temperature of the outer surface of the tank as a variable, which is not yet known. The convective heat transfer, Q_2 , can be found using equations [11] and [12] in addition to equations [5-7] or equations [8-10] for forced and natural convection, respectively. Again, the temperature of the outer surface of the tank is left as a variable. From conservation of energy $Q_1 + Q_2 + Q_3 = Q_4$. The temperature of the outer surface of the tank can be found with this equation. The equivalent resistance of the system of the tank outer shell, mylar layer, and insulation layer can then be found from equation [1]. Since the individual resistances of the outer shell and mylar layer can be found from equation [2], the individual resistance of the insulation layer can then be found from equation [13]. Finally, equation [2] can be used to find the thickness of the insulation layer. Additionally, the weight of the required insulation can be found by multiplying the density of the insulation material by the surface area of the tank and the found required thickness of insulation.

In the case that the fuel usage is gaseous, a boiloff rate equivalent to the idle fuel usage rate is allowed. Essentially, the insulation should be designed to allow the amount of heat transfer that causes the hydrogen to evaporate at a minimum of the idle fuel usage rate, so that no internal heating is required to produce the gaseous hydrogen for the fuel lines at idle. In this case, all evaporation that is below the idle fuel usage rate is no longer considered “boiloff” since it is desired.

Results

The calculated plots of boiloff rate vs. insulation thickness for EPS, MLI, and Glass Bubbles insulations at cruise conditions with liquid hydrogen fuel usage and a full tank are shown in Figure 5.

Lines representing 20%, 50%, and 100% of the idle fuel usage rate have been added to give context to the boiloff rate axis.

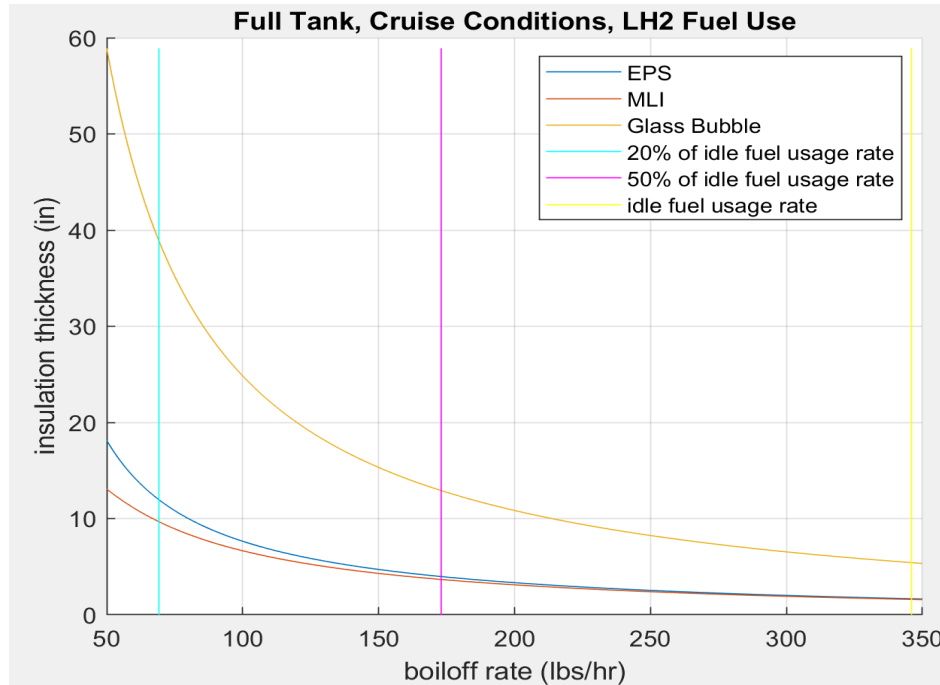


Figure 5: Boiloff rate vs. insulation thickness for EPS, MLI, and Glass Bubbles insulations at cruise conditions with various liquid hydrogen fuel usage rate.

The boiloff rate has been cut off at 50 lbs. /hr so that the plot is more readable. At values less than 13 lbs. /hr , the calculated insulation thicknesses become negative (not realistic), signifying that it is not possible to prevent 13 lbs. /hr of boiloff with the chosen placement of insulation. This is because the lugs conduct heat straight to the inner structural shell, bypassing the insulation layer. Unfortunately, this is unavoidable since the lugs need to be structurally connected to the inner tank shell to secure the tank safely to the plane wing. Thin layers of nylon insulation have been added into the design of the lugs to limit the conduction through them. Overall, 13 lbs. /hr of boiloff is not a very big loss, since it is only about 4% of the idle fuel usage rate. Between the boiloff rates of 13 lbs. /hr and 50 lbs/hr, the insulation thicknesses spike to unreasonably large values that increase the chart axes to the point that the rest of the data is hard to distinguish.

As expected, Figure 5 shows an inverse relationship between insulation thickness and boiloff rate. Smaller insulation thicknesses correspond with higher boiloff rates and larger insulation thicknesses correspond to lower boiloff rates. The relationship is nonlinear and appears more similar to $y=1/x$ relationship. This means that increasing the insulation thickness from smaller values initially has a

large impact on boiloff rate, but as the thickness gets larger, increasing it has less effect on the boiloff rate.

Glass Bubbles insulation has the largest required insulation thicknesses of the three insulation materials, and MLI has the smallest. This makes sense since Glass Bubbles insulation has the highest thermal conductivity and MLI has the lowest. In fact, the required insulation thickness has an approximately linear relationship with thermal conductivity. Glass Bubbles insulation has a thermal conductivity approximately 5 times greater than EPS.^{7,3} At a boiloff rate equal to 20% of the idle fuel usage rate, Glass Bubbles insulation has a required insulation thickness approximately 5 times greater than EPS. This makes sense in the context of the model since a vast majority of the heat transfer into the tank occurs through the layer of insulation, and conduction through insulation has a linear relationship with thickness and thermal conductivity, as shown in equation [2]. This relationship is hard to show for MLI since MLI's thermal conductivity is considered variable in this model.

In the case that the fuel usage will be gaseous, all evaporation below the idle fuel usage rate is not considered to be "boiloff" since it is desired. The first 346 lbs. /hr (CFM56-7B24 engine idle fuel usage rate) of evaporation is disregarded from the boiloff rate. The plots of boiloff rate vs. insulation thickness are the same as in the case of liquid fuel usage in Figure 5, except the correspondence is shifted linearly by the value of the boiloff rate, e.g. a thickness that corresponded to 346 lbs. /hr in the liquid fuel usage case now corresponds to a 0 lbs. /hr boiloff rate. These plots are shown in Figure 6.

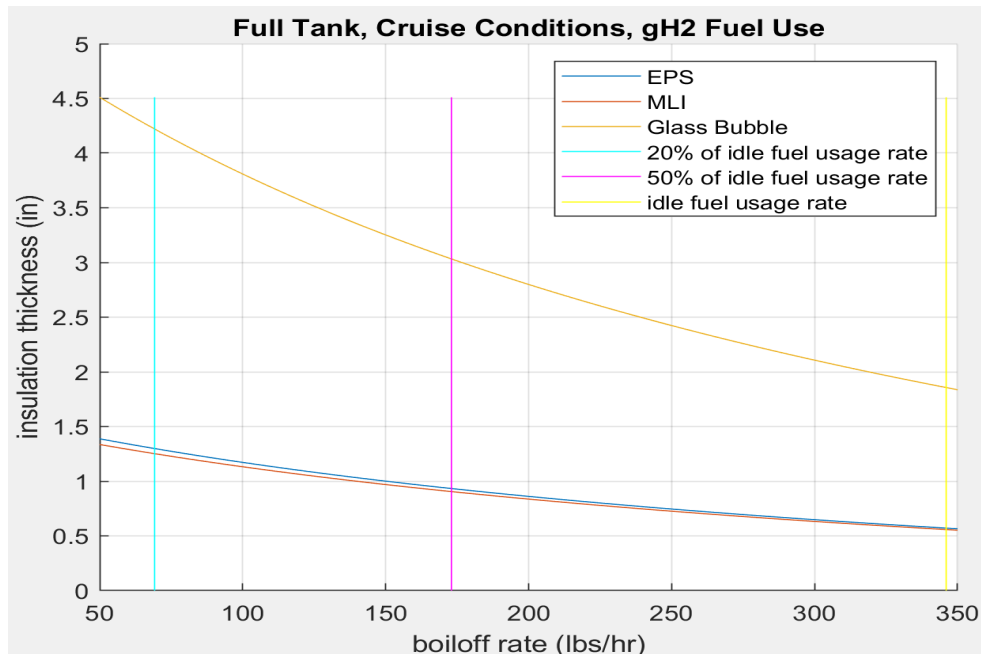


Figure 6: Boiloff rate vs. insulation thickness for EPS, MLI, and Glass Bubbles insulations at cruise conditions with various gaseous hydrogen fuel usage rate

To limit the “boiloff” (not including the 346 lbs. /hr of evaporation that goes towards gaseous fuel usage) to 20% of the idle fuel usage rate, only 4.22” of Glass Bubbles insulation, 1.30” of EPS, or 1.25” of MLI is required.

The calculated plots of boiloff rate vs. insulation thickness for EPS, MLI, and Glass Bubbles insulations at on-ground idle conditions with liquid hydrogen fuel use and a full tank are shown in Figure 7.

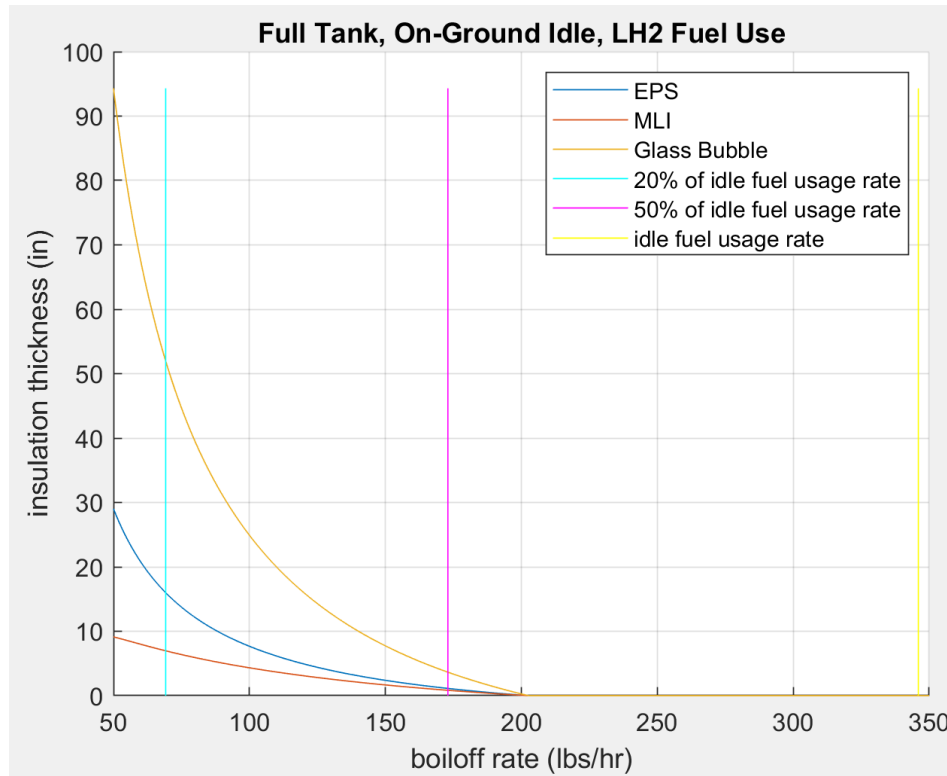


Figure 7: Boiloff rate vs. insulation thickness for EPS, MLI, and Glass Bubbles insulations at on-ground idle conditions with various liquid hydrogen fuel usage rate

The boiloff rate is cut off below 50 lbs. /hr since the conductive heat transfer through the lugs causes a boiloff rate of 39 lbs. /hr. This is greater than the boiloff rate it causes during cruise because the temperature of the plane body is greater on the ground than in flight. Above the boiloff rate of 220 lbs. /hr, the insulation thicknesses for all materials are 0. This is because, given the rest of the tank structure and the conditions on the ground, the amount of heat transfer cannot exceed the amount that causes 220 lbs. /hr of boiloff, even without any insulation.

The calculated plots of boiloff rate vs. insulation thickness for EPS, MLI, and Glass Bubbles insulations at cruise conditions with liquid hydrogen fuel usage and a 95% empty tank are shown in Figure 8.

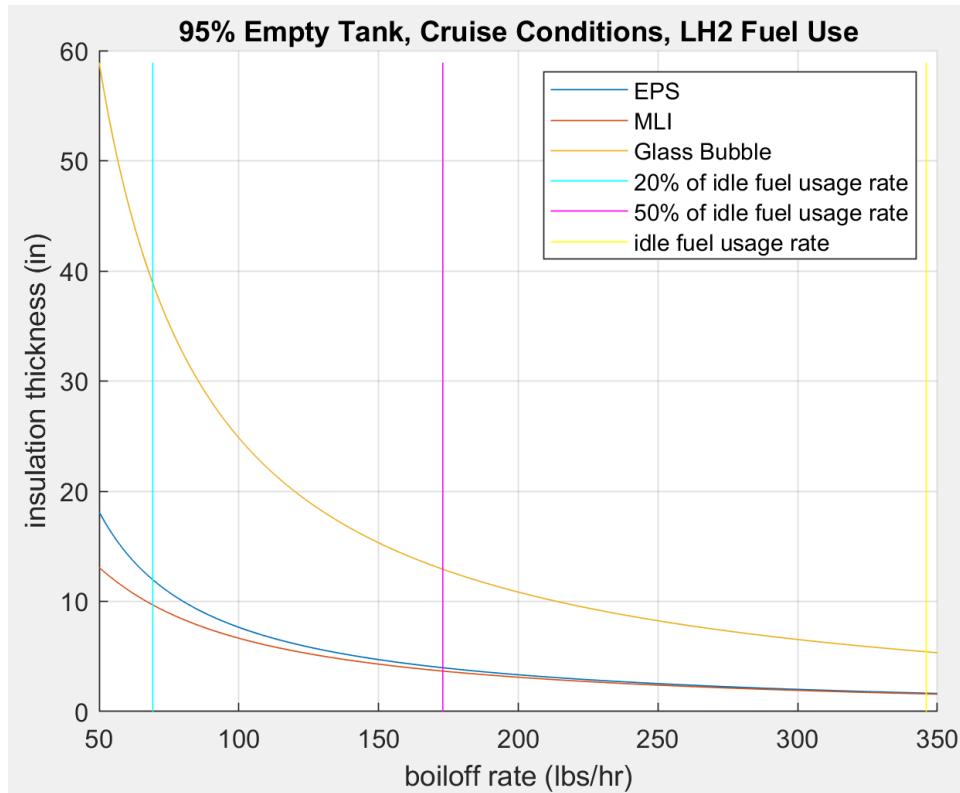


Figure 8: Boiloff rate vs. insulation thickness for EPS, MLI, and Glass Bubbles insulations in cruise condition with 95% empty tank for various liquid hydrogen fuel usage rate

The plots in Figure 8 are almost identical to the one for cruise conditions, liquid hydrogen fuel use, and a full tank in Figure 5. No visible differences are noticeable.

The Table below compares the required thicknesses and weights of EPS in the four cases presented in Figures 5-8.

		20% of idle fuel usage	50% of idle fuel usage	100% of idle fuel usage
Cruise, LH2 Fuel Use, Full Tank	Thickness (in)	12.01	3.97	1.67
	Weight (lbs.)	1,887	624	262
Ground Idle, LH2 Fuel Use, Full Tank	Thickness (in)	8.06	1.37	0
	Weight (lbs.)	2,450	191	0
Cruise, gH2 Fuel Use, Full Tank	Thickness (in)	1.30	0.933	0.571
	Weight (lbs.)	204	147	90.0
Cruise, LH2 Fuel Use, 95% Empty Tank	Thickness (in)	12.01	3.97	1.67
	Weight (lbs.)	1,887	624	262

The values of thickness and weight for cruise condition with liquid fuel use and a full and almost empty tank are equal. This shows that the fullness of the tank has negligible effect on the required thickness or weight of insulation. This is reasonable since we have assumed that all the liquid and gaseous hydrogen will be at the critical temperature throughout the process.

The gaseous fuel use case requires less thickness and weight than the liquid fuel usage case, which is expected since the gaseous fuel use case allows 346 lbs./hr of evaporation in addition to the boiloff rate.

The cruise condition requires greater thicknesses and weights than the ground idle condition. This implies that the forced convection during cruise causes the most significant heat transfer compared to the radiation from the atmosphere, radiation from the sun, and conduction through the lugs.

For the limiting case of cruise conditions and liquid fuel usage, a table summarizing the thicknesses and weights of different insulation materials required to limit the boiloff rate to 20%, 50%, and 100% of the idle fuel usage rate is shown below.

		20% of idle fuel usage	50% of idle fuel usage	100% of idle fuel usage
EPS	Thickness (in)	12.0	3.97	1.67
	Weight (lbs.)	1,890	624	262
MLI	Thickness (in)	9.70	3.70	1.60
	Weight (lbs.)	10,100	3,840	1,670
Glass	Thickness (in)	39.0	12.9	5.42
Bubbles	Weight (lbs.)	54,300	18,000	7,540

As previously mentioned, the required thickness of insulation has an approximately linear relationship with the thermal conductivity; hence Glass Bubbles insulation has both a thermal conductivity and required insulation thickness approximately 5 times greater than EPS.^{7,3}

Conclusions and Future Work

The worst case from a boiloff rate perspective is when the plane is cruising, since the forced convection during flight causes the most significant amount of heat transfer. The fullness of the tank has negligible effect on the boiloff rate. MLI is the most effective insulating material, but it has higher density than EPS, therefore it requires smaller thicknesses but greater weights of insulation than EPS. MLI also has a number of drawbacks. First, it is still a very new technology which has not been fully developed for mass production. Additionally, there is a lack of data on its thermal performance that causes some ambiguity as to its true thermal conductivity. Some studies have shown that MLI is

significantly less insulating effect at colder temperatures, since it was originally designed for reflecting high heat.⁴ Lastly, MLI is very expensive. For these reasons, EPS seems to be the best material since it is cheap and well proven and requires the least weight to maintain given boiloff rates.

The usage of gaseous hydrogen for the fuel line significantly reduces the required insulation thickness since a minimum of 346 lbs./hr of evaporation is allowed. However, it is risky to design the insulation with this plan in mind since there will inevitably be times when the plane is on the ground and the engine is not running at all, for example overnight. If the engine is not running, no fuel is being used, therefore allowing the tank to boiloff at 346 lbs./hr or greater will cause major pressurization and safety issues. One way to combat this could be to have a special system for overnight handling of the plane in which an external refrigeration system is used to cool the tank, or the hydrogen could be released from the tank and stored in a more insulated external tank. There is a tradeoff between reducing the thickness and weight of insulation required and managing the boiloff rate overnight; perhaps a compromised could be achieved.

Overall, using 3.97 inches (624 lbs.) of EPS per tank to limit the boiloff rate to 50% of the idle fuel usage rate during the worst-case scenario is physically reasonable. It is neither the size nor weight that would cause the plane to no longer be able to fly, or significantly reduce the plane’s efficiency.

The future work for this study will include a three-dimensional heat transfer simulation analysis using the current tank structure design in COMSOL.

Appendix A: Values of Various Variables Used

A Table of all values used in this study as well as their sources is given below:

Variable	Value
Absorptivity of white paint on outer shell ⁸	0.02
Temperature of the sky/air at 35,000 ft ⁹	218.9 K
Density of air at 35,000 ft ⁹	0.38035 kg/m ³
Dynamic viscosity of air at 35,000 ft ⁹	1.39*10 ⁻⁵ kg*s/m ²
Heat capacity of air at 35,000 ft ¹⁰	1.002 kJ/kg*K
Diameter of outside of tank	1.939 m
Length of tank	16.76 m
Solar irradiation ¹¹	1,367 W/m ²
Saturation temperature for normal hydrogen at 95 psi (design tank pressure) ¹²	28.7 K

Enthalpy of saturated liquid normal hydrogen at 95 psi ¹²	114.55 kJ/kg
Enthalpy of saturated vapor hydrogen at 95 psi ¹²	452.51 kJ/kg
Carbon epoxy thickness	0.00127 m
Carbon epoxy thermal conductivity ¹³	0.15 W/m*K
Mylar thickness	25.4*10 ⁻⁶ m
Mylar thermal conductivity ¹⁴	0.14 W/m*K
Aluminum thermal conductivity ¹⁵	225.94 W/m*K
Structural shell thickness	0.001778 m
Nylon thermal conductivity ¹⁶	0.25 W/m*K
Fuel usage rate at cruise	829 lbs/hr
Fuel usage rate at CFM56-7B24 10% idle	346 lbs/hr
Plane speed at cruise	232 m/s
EPS spray on foam thermal conductivity ³	0.02594 W/m*K
Calculated forced convection coefficient	3.10 W/m ² K
Temperature of the sky/air at sea level on a hot day	120 F
Density of air at sea level on a hot day ¹⁷	1.097 kg/m ³
Dynamic viscosity of air at sea level on a hot day ¹⁸	1.95*10 ⁻⁵ kg*s/m ²
Heat capacity of air at sea level on a hot day ¹⁹	1007 J/kg*K
Prandtl number of air at sea level on a hot day ²⁰	0.705
Thermal expansion coefficient of air at sea level on a hot day ²¹	0.00312 K ⁻¹
EPS spray on foam density ³	1.6229 lbs/ft ³
MLI thermal conductivity ⁶	0.135*10 ⁻³ W/m*K
MLI density ²²	10.8 lbs/ft ³
Glass Bubbles thermal conductivity ⁷	0.130 W/m*K
Glass Bubbles density ⁷	14.36 lbs/ft ³

References

1. Assets.publishing.service.gov.uk.
https://assets.publishing.service.gov.uk/government/uploads/system/uploads/attachment_data/file/1059938/_CP_605___National_Shipbuilding_Strategy_Refresh_100322.pdf.
2. Bergman, Theodore, and Adrienne Lavine. Fundamentals of Heat and Mass Transfer, Seventh Edition Binder Ready Version. John Wiley and Sons, 2011.

3. Gnip, Ivan, et al. "Thermal Conductivity of Expanded Polystyrene (EPS)." Researchgate.net, 2012, https://www.researchgate.net/publication/257227323_Thermal_conductivity_of_expanded_polystyrene_EPS_at_10_C_and_its_conversion_to_temperatures_within_interval_from_0_to_50_C.
4. "Quantifying MLI Thermal Conduction in Cryogenic ..." Quantifying MLI Thermal Conduction in Cryogenic Applications from Experimental Data, CalTech Jet Propulsion Laboratory, https://www2.jpl.nasa.gov/adv_tech/coolers/Cool_ppr/CEC2015%20Quantifying%20MLI%20Thermal%20Conduction.pdf.
5. Hurd, Joseph A. "Multilayer Insulation Testing at Variable Boundary Temperatures." Florida State University, 2013.
6. Deng, Bikai, et al. "Study of the Thermal Performance of Multilayer Insulation Used in Cryogenic Transfer Lines." Cryogenics, Elsevier, 24 Jan. 2019, <https://www.sciencedirect.com/science/article/abs/pii/S0011227518302777>.
7. "3M™ Glass Bubbles for Buoyancy and Thermal Insulation." 3M Multimedia, <https://multimedia.3m.com/mws/media/6313770/3mtm-glass-bubbles-for-buoyancy-and-thermal-insulation.pdf>.
8. Rice, Doyle. "Scientists Created the World's Whitest Paint. It Could Eliminate the Need for Air Conditioning." USA Today, Gannett Satellite Information Network, 30 Sept. 2021, <https://www.usatoday.com/story/news/nation/2021/09/17/whitest-paint-created-global-warming/8378579002/>.
9. "U.S. Standard Atmosphere vs. Altitude." Engineering ToolBox, https://www.engineeringtoolbox.com/standard-atmosphere-d_604.html.
10. Specific Heat Capacities of Air - (Updated 7/26/08), https://www.ohio.edu/mechanical/thermo/property_tables/air/air_Cp_Cv.html.
11. Introduction to Solar Radiation, <https://www.newport.com/t/introduction-to-solar-radiation>.
12. Leachman, J. W., et al. "Fundamental Equations of State for Parahydrogen, Normal Hydrogen, and Orthohydrogen." Journal of Physical and Chemical Reference Data, vol. 38, no. 3, 2009, pp. 721–748., <https://doi.org/10.1063/1.3160306>.
13. Thermal Properties of Carbon Fiber-Epoxy Composites with ... https://www.researchgate.net/profile/Ronald-Joven/publication/288102626_Thermal_properties_of_carbon_fiber-epoxy_composites_with_different_fabric_weaves/links/56be27e408aee5caccf2f5d3/Thermal-properties-of-carbon-fiber-epoxy-composites-with-different-fabric-weaves.pdf.
14. "Mylar Thermal Insulating Film, 304mm x 200mm x 0.05mm." MYLAR FILM 304X200X0.05MM | Mylar Thermal Insulating Film, 304mm x 200mm x 0.05mm | RS Components, <https://se.rs-online.com/web/p/thermal-insulating-films/5365986>.
15. "Materials Database - Thermal Properties." Thermtest Inc., 14 Oct. 2020, <https://thermtest.com/thermal-resources/materials-database>.
16. "Plastics - Thermal Conductivity Coefficients." Engineering ToolBox, https://www.engineeringtoolbox.com/thermal-conductivity-plastics-d_1786.html.
17. "Air - Density, Specific Weight and Thermal Expansion Coefficient vs. Temperature and Pressure." Engineering ToolBox, https://www.engineeringtoolbox.com/air-density-specific-weight-d_600.html.
18. "Air - Dynamic and Kinematic Viscosity." Engineering ToolBox, https://www.engineeringtoolbox.com/air-absolute-kinematic-viscosity-d_601.html.
19. "Air - Specific Heat vs. Temperature at Constant Pressure." Engineering ToolBox, https://www.engineeringtoolbox.com/air-specific-heat-capacity-d_705.html.

20. "Air - Prandtl Number." Engineering ToolBox, https://www.engineeringtoolbox.com/air-prandtl-number-viscosity-heat-capacity-thermal-conductivity-d_2009.html.
21. "Air - Density, Specific Weight and Thermal Expansion Coefficient vs. Temperature and Pressure." Engineering ToolBox, https://www.engineeringtoolbox.com/air-density-specific-weight-d_600.html.
22. Deng, Bicaï, et al. "Study of the Thermal Performance of Multilayer Insulation Used in Cryogenic Transfer Lines." *Cryogenics*, Elsevier, 24 Jan. 2019, <https://www.sciencedirect.com/science/article/abs/pii/S0011227518302777#:~:text=The%20results%20indicated%20that%20the,achieved%20as%20an%20adequate%20specimen>.